

# Meta-modelling of deep rolling process of train axles (auxiliary online material)

Z. Dombovari<sup>a</sup>, L. Galdos<sup>b</sup>, R. Merino<sup>c</sup>, A. Szlancsik<sup>d</sup>, K. Bobor<sup>d</sup>, G. Henap<sup>e</sup>, G. Stepan (1)<sup>e</sup>, J. Munoa (1)<sup>c</sup>

<sup>a</sup> MTA-BME Lendület Machine Tool Vibration Research Group, Department of Applied Mechanics, Budapest University of Technology and Economics, Budapest, Hungary

<sup>b</sup> Department of Mechanical and Industrial Production, Mondragon Unibersitatea Elgoibar, Mondragon, Basque Country, Spain

<sup>c</sup> Ideko – Member of BRTA, Dynamics & Control, Elgoibar, Basque Country, Spain

<sup>d</sup> Department of Materials Science and Engineering, Budapest University of Technology and Economics, Budapest, Hungary

<sup>e</sup> Department of Applied Mechanics, Budapest University of Technology and Economics, Budapest, Hungary

Surrogate analytical model was developed and validated for axles (deep) rolling. This is an important cold-forming process to ensure compressive residual stress field in the surface layer to increase the lifetime of e.g., train axles. Two independent distinct finite element models were developed that can simulate the time evolution and directly the stationary solution of this forming process. Important feed dependency was recognized causing maximum forming force with respect to the applied feed. A 'lower' and a 'higher force' measurement setup were developed for validation carried out by measuring surface features and residual stresses.

Cold forming, Rolling, Finite element method (FEM), Chatter

## 1. Meta-modelling and experimental validation

Even though all finite element (FE) calculations were performed in a  $\delta$ -driven manner, to measure accurately enough during operation the relative distance between the axle and the roller is extremely difficult. The indentation is very small, and often on or below the static deflection of the machine, which was truly beyond of reach. In contrast, forming force  $F$  can be measured and controlled online relatively easily with a great accuracy and repeatability. This allows simple  $F$ -driven tests to be performed, however, these two  $\delta$ - &  $F$ -driven considerations are not compatible. Unlocking this, one of the set (FE) must be enlarged ( $i$ ) and inverted back from  $F(\delta;f)=F_j$  to  $\delta_i=\delta(F_j;f)$ , where  $\delta_i$  are determined after the operation. This means the  $f$ - $F$  characteristics can be validated if  $F(\delta;f)$  and  $\delta(F;f)$  analytical meta-functions are known. The functions were defined as product

$$\diamond(\delta, f, r, R) := \diamond_\delta(\delta) \times \diamond_f(f) \times \diamond_r(r) \times \diamond_R(R), \quad (1)$$

of rational fractional polynomials with various orders, where  $\diamond$  is  $F$ ,  $\bar{\varepsilon}_p$  or  $\delta_R$ . The quality of the meta-model (MM) fitting (differential evolution / interior point) on 'complete implicit time simulation' ITS(Marc) / 'quasi-static prescribed displacement calculation' PDC(Ansys). Slow ITS is only delivering result in (hybrid) sparse points over latin-cube and some single parameter equidistant sampling providing ( $\delta - F$ ) and ( $f - F$ ). Fast PDC giving data for testing the fitting on hybrid latin-cube sampling comparing with its own extensive equidistant parameter scanning.

The construction of the functions were performed heuristically by taking into account their specific behaviour. For example, in the determined FE points it was clear somehow the elastic plastic relay must be treated. Or the clearly visible extremum in the feed direction.

In this regard the indentation dependency  $\delta$  was dealt with piecewise smooth polynomial function shown below:

$$\diamond_\delta(\delta) := (1 - H(\delta, \delta_S)) \frac{\sum_{k=0}^1 \diamond_{n,\delta 1,k}}{\diamond_{d,\delta 1,0}} + H(\delta, \delta_S) \frac{\sum_{k=0}^3 \diamond_{n,\delta 2,k}}{\diamond_{d,\delta 2,0}}. \quad (2)$$

While the extremum in the feed  $f$  direction was determined by a rational polynomial function as

$$\diamond_f(f) := \frac{\sum_{k=0}^4 \diamond_{n,f,k}}{\sum_{k=0}^3 \diamond_{d,f,k}} \quad (3)$$

Simple low order dependency was expected with the outer radius  $R$  and meridian (nose) radius  $r$  of the roller.

$$\diamond_r(r) := \frac{\sum_{k=0}^3 \diamond_{n,r,k}}{\diamond_{d,r,0}} \quad (4)$$

$$\diamond_R(R) := \frac{\sum_{k=0}^3 \diamond_{n,R,k}}{\diamond_{d,R,0}} \quad (5)$$

Since it was a specific problem for a given train axle we had chosen the train axle to be  $D=152\text{mm}$  for the entire set of point to remove one additional parameter from the optimization.

### 1.1. $F(\delta, f, r, R)$ fitted on ITS results

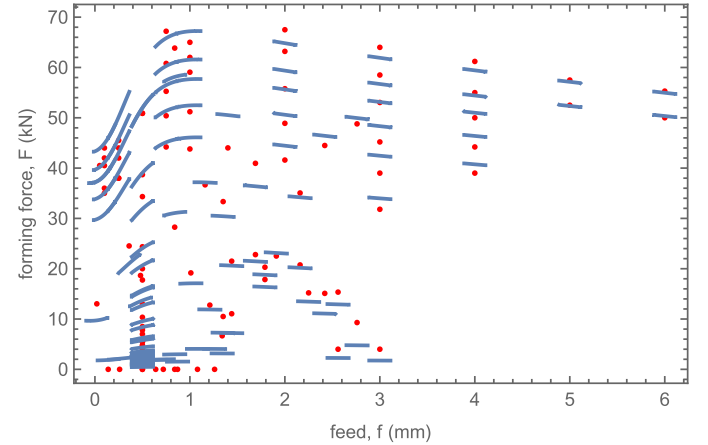


Figure 1. shows foliated result for  $f$ - $F(\delta, f, r, R)$  ITS results

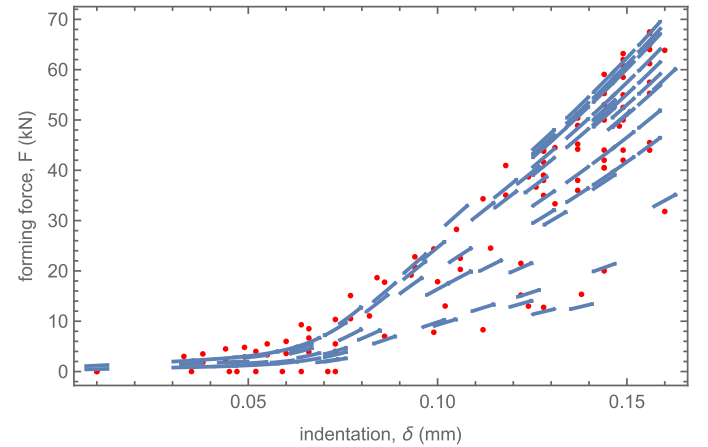
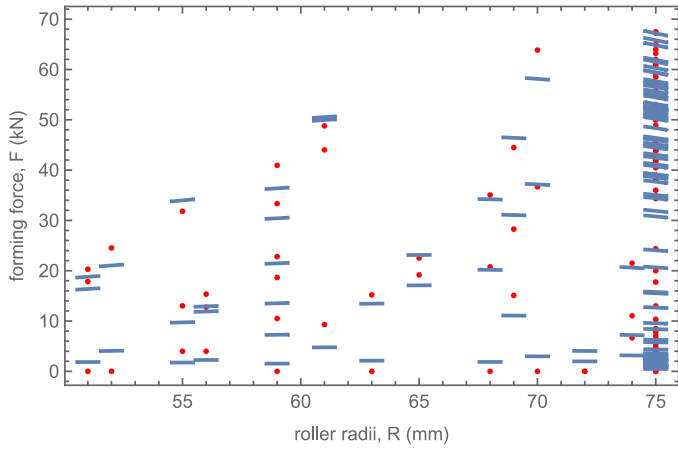
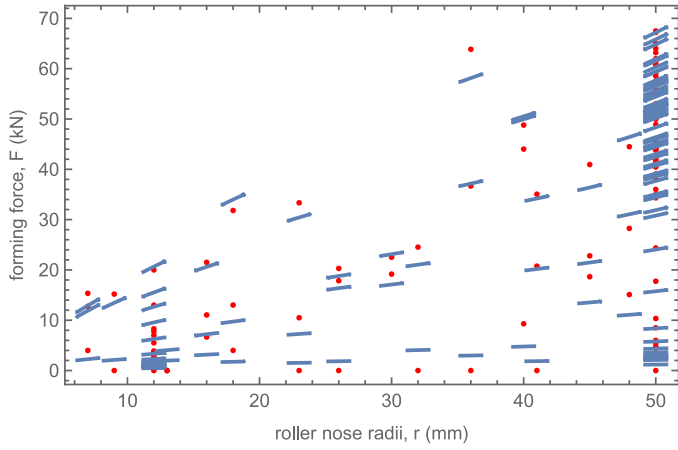


Figure 2. shows foliated result for  $\delta$ - $F(\delta, f, r, R)$  ITS results



**Figure 3.** shows foliated result for  $R\text{-}F(\delta, f, r, R)$  ITS results



**Figure 4.** shows foliated result for  $r\text{-}F(\delta, f, r, R)$  ITS results

## 1.2. $\bar{\epsilon}_p(\delta, f, r, R)$ fitted on ITS results

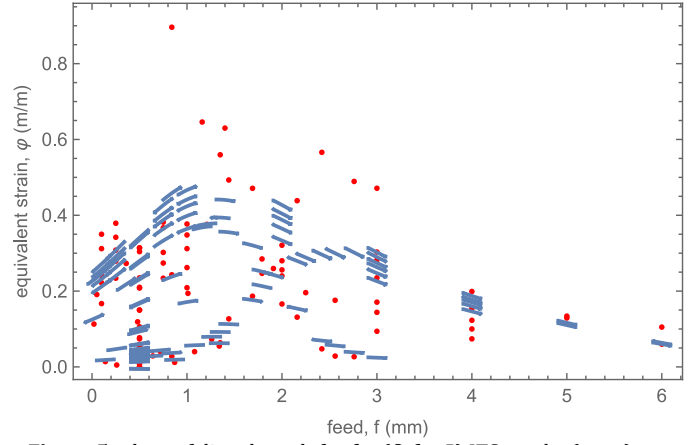


**Figure 5.** shows foliated result for  $f\text{-}\bar{\epsilon}_p(\delta, f, r, R)$  ITS results ( $\varphi=\bar{\epsilon}_p$ )

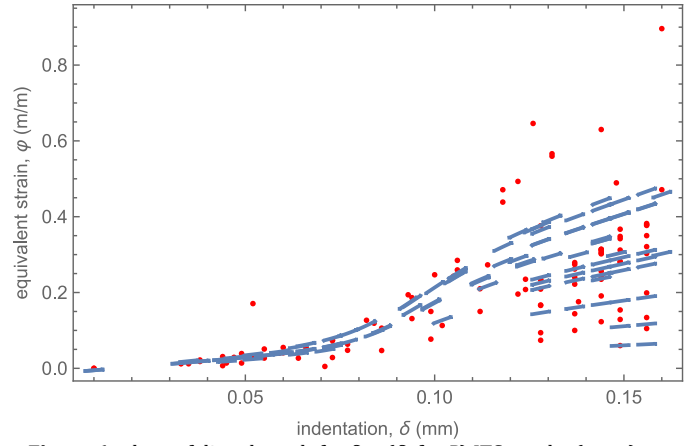


**Figure 6.** shows foliated result for  $\delta\text{-}\bar{\epsilon}_p(\delta, f, r, R)$  ITS results ( $\varphi=\bar{\epsilon}_p$ )

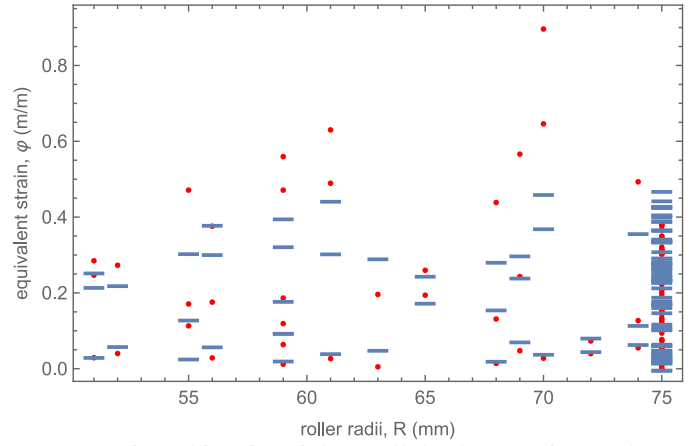


**Figure 7.** shows foliated result for  $R\text{-}\bar{\epsilon}_p(\delta, f, r, R)$  ITS results ( $\varphi=\bar{\epsilon}_p$ )

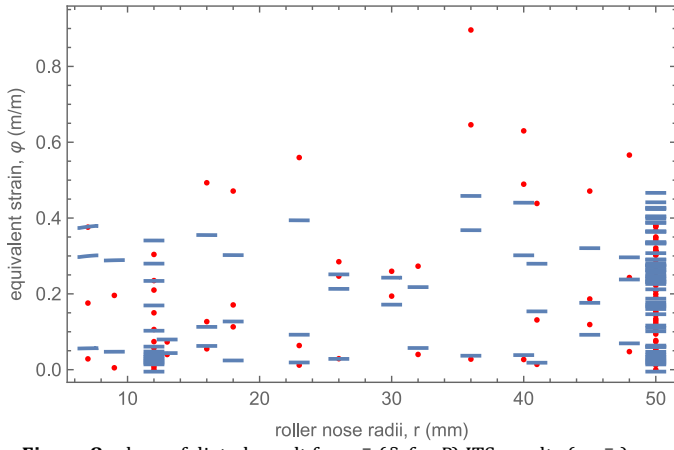


**Figure 8.** shows foliated result for  $r\text{-}\bar{\epsilon}_p(\delta, f, r, R)$  ITS results ( $\varphi=\bar{\epsilon}_p$ )

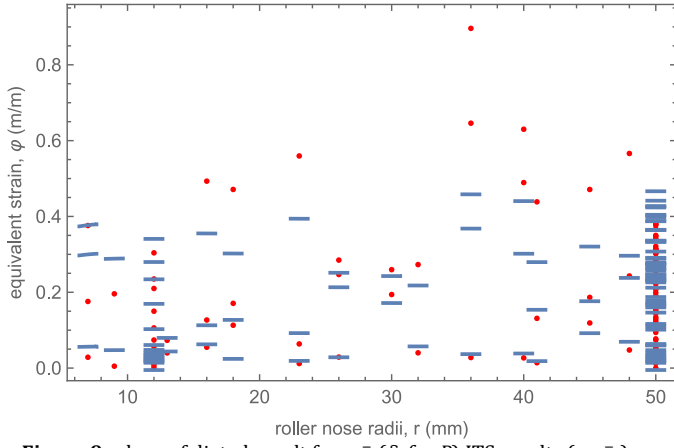


**Figure 9.** shows foliated result for  $r\text{-}\bar{\epsilon}_p(\delta, f, r, R)$  ITS results ( $\varphi=\bar{\epsilon}_p$ )

### 1.3. $\delta_R(\delta, f, r, R)$ fitted on ITS results

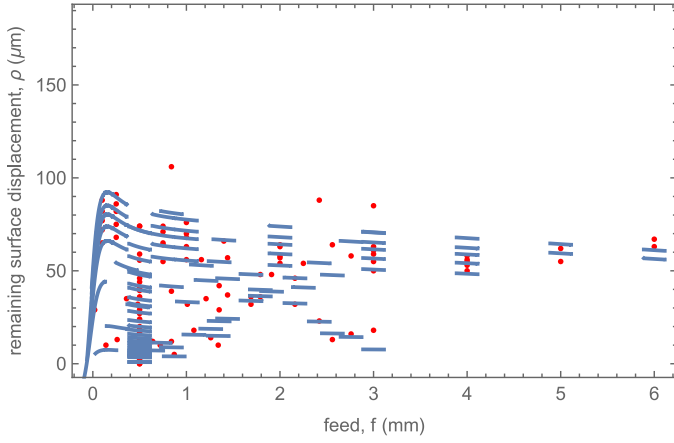


**Figure 10.** shows foliated result for  $f\text{-}\delta_R(\delta, f, r, R)$  ITS results ( $\rho=\delta_R$ )

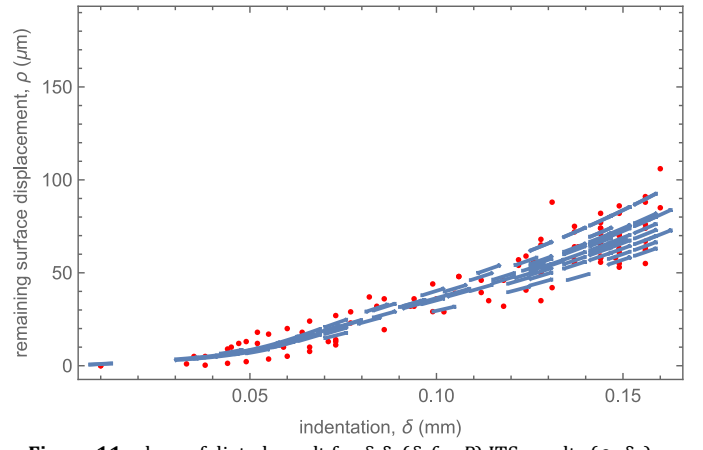


**Figure 11.** shows foliated result for  $\delta\text{-}\delta_R(\delta, f, r, R)$  ITS results ( $\rho=\delta_R$ )

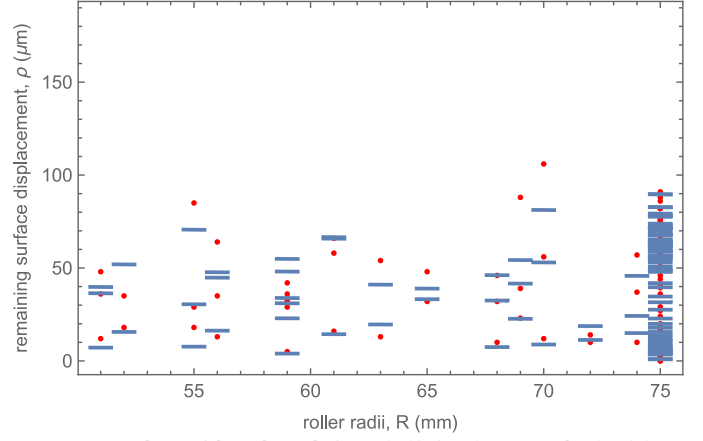


**Figure 12.** shows foliated result for  $R\text{-}\delta_R(\delta, f, r, R)$  ITS results ( $\rho=\delta_R$ )

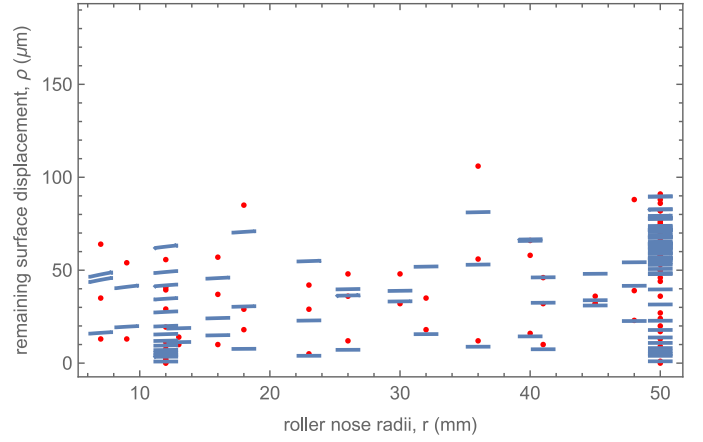


**Figure 13.** shows foliated result for  $R\text{-}\delta_R(\delta, f, r, R)$  ITS results ( $\rho=\delta_R$ )